

## A Histological Study of the Impact of Bone Marrow Mesenchymal Stem Cells- Derived Exosomes on the Corpus Callosum in a Cuprizone-Induced Mouse Model of Multiple Sclerosis

*Bosy Ahmed Abdelaziz Hassan, Nagwa Mohamed El Shakaa, Gehad Ahmed Hammouda and Mona Hussien Raafat Ahmed*

*Department of Histology, Faculty of Medicine, Ain Shams University, Cairo, Egypt*

### ABSTRACT

**Introduction:** A chronic demyelinating disease that affects millions of peoples worldwide is multiple sclerosis (MS). There are currently no remyelination therapy for this disease, and exosomes are being explored as an alternative.

**Aim of the Work:** To study how exosomes generated from bone marrow mesenchymal stem cells (BMSCs) affect the corpus callosum structure in male mice with cuprizone model of MS.

**Materials and Methods:** Forty-seven adult male mice were used in this work. Exosomes were isolated and extracted from five mice. Forty-two adult male mice were split into two equal groups randomly: Group I (Control): divided into three equal subgroups. Group II (Cuprizone-treated): which was treated with cuprizone, was given 400 mg/kg/day of the drug orally every day for 8 weeks. Then equally divided into three subgroups. Subgroup IIA: sacrificed 24 hours following the final cuprizone dosage. Subgroup IIB (Recovery): left without treatment for further 4 weeks, then were sacrificed. Following the final dose of cuprizone, subgroup IIC (exosomes treated): got a single intravenous injection of exosomes into tail vein, and were sacrificed 4 weeks later. After scarification, brains tissue were prepared using histological, immune-histochemical methods and histomorphometric studies.

**Results:** Histological analysis of corpus callosum in subgroups IIA & IIB showed damaged nerve fibers by H&E with multiple vacuoles. Improvement of these changes was noticed in subgroup IIC. By luxol fast blue, nerve fibers stained deep blue in subgroup IIC & control group. While, in subgroups IIA & IIB, nerve fibers stained faint blue. Subgroups IIA & IIB showed marked rise in the number of GFAP and Iba1 positive cells.

**Conclusions:** In the cuprizone model of MS, exosomes were demonstrated to improve demyelination of mice's corpus callosum. Exosomes may therefore offer a novel approach to MS treatment.

**Received:** 16 March 2025, **Accepted:** 23 March 2025

**Key Words:** BMSCs derived exosomes, Corpus callosum, Cuprizone, GFAP, MS.

**Corresponding Author:** Bosy Ahmed Abdelaziz Hassan, MD, Department of Histology, Faculty of Medicine, Ain Shams University, Cairo, Egypt, **Tel.:** +20 10 9998 5034, **E-mail:** bosyhany132013@yahoo.com

**ISSN:** 1110-0559, Vol. 48, No. 2

### INTRODUCTION

The central nervous system (CNS) is frequently affected by multiple sclerosis (MS), a demyelinating illness that affects both the white and gray matter. It is regarded as a major contributor to young adults' non-traumatic disabilities<sup>[1,2]</sup>.

Toxic demyelination in rodents is induced by the copper-chelating chemical cuprizone. It inhibits the copper-dependent enzymes of the mitochondria. A number of metalloenzymes use copper as a catalytic co-factor, thus, cuprizone is crucial to the central nervous system's physiology<sup>[3]</sup>. Mojaverrostami *et al.* reported that cuprizone-induced demyelination by promoting mature oligodendrocytes apoptosis associated with astrocytes and microglial cell activation<sup>[4]</sup>.

Several studies focused on cell-free therapy including extracellular vesicles as exosomes and micro-vesicles<sup>[5]</sup>.

Extracellular vesicles (EVs) play an important role in cell-to-cell communication. They are membrane-bound particles secreted by cells and categorized based on to their size and biogenesis<sup>[6]</sup>. Exosomes are considered the smallest extracellular vesicles with an estimated size that ranges between 30 and 150 nm in diameter<sup>[6]</sup>. They are strong candidates for treating CNS diseases because they can pass through the blood-brain barrier (BBB)<sup>[7]</sup>. Several studies suggested that EVs exhibit anti-inflammatory effects, lower quantity of activated inflammatory microglial cells, support oligodendrocytes and protect neurons<sup>[1,8]</sup>.

### AIM OF THE WORK

The present work aimed to identify the possible therapeutic impact of exosomes produced from BMSCs on the corpus callosum of adult male mice with multiple sclerosis in the cuprizone model.

## MATERIALS AND METHODS

### Materials

#### Drugs

Cuprizone Oxalic acid, bis (cyclohexylidenehydrazide), 98% (code:154421000), MW=278,34 C<sub>14</sub> H<sub>22</sub>N<sub>4</sub> O<sub>2</sub>, was given daily to mouse at a dose of 400 mg/kg/day<sup>[9]</sup> orally for 8 weeks. Cuprizone was purchased from Across Organics, Janssen Pharmaceuticaaan 3a, B-2440 Geel, Belgium. It was received as a whitish powder in a 100 gm package.

#### Preparation and characterization of Exosomes

Exosomes were extracted using ultracentrifugation from mesenchymal stem cells derived from bone marrow (BMSCs). After three passages of culturing BMSCs, when tissue culture flasks reached 70-80% confluence, conditioned media were collected in 50ml centrifuge tubes. The collected media was centrifuged, using a cooling centrifuge (Centurion Scientific K2015 R Centrifuge, UK), at >1000 xg for 10 minutes at 4°C to get rid of any residual cells. Then, the pellet was discarded, and the supernatant was transferred to a new centrifuge tube. After that, samples were centrifuged for 20 minutes at 4°C at 2000–5000 xg using a cooled centrifuge to remove big debris and dead cells. The supernatant was then moved to a fresh centrifuge tube, and the pellet was disposed of. A 0.22 µm filter (CHMLAB Group, Spain) was used to remove any remaining cellular debris from the supernatant. After filtering, the sample was put into an ultracentrifuge tube and centrifuged for one hour at 100,000 xg using a Sorval-MTx150, USA ultracentrifugation machine. The small EVs were found in the collected pellet, whereas the supernatant was disposed of. The pellet was kept at -80 until it was needed and was immediately resuspended in 100 µm PBS, or phosphate buffer saline<sup>[10,11]</sup>. Purified exosome concentrate was obtained by ultracentrifugation of conditioned media of 1×10<sup>6</sup> BMSCs in 0.1 ml PBS. Preparation of BMSCs was done in the Histology Department's Stem Cell Research Unit at Ain Shams University's Faculty of Medicine while isolation of exosomes by Ultracentrifugation was done at the National Research Center, Cairo, Egypt. Characterization of exosomes<sup>[12]</sup> was done using transmission electron microscopy (TEM), JEOL- 1010; 80kv, at The Regional Center for Mycology and Biotechnology (RCMB), Al-Azhar University. Exosomes appeared as membrane-bound vesicles with variable diameters (Figure 1).

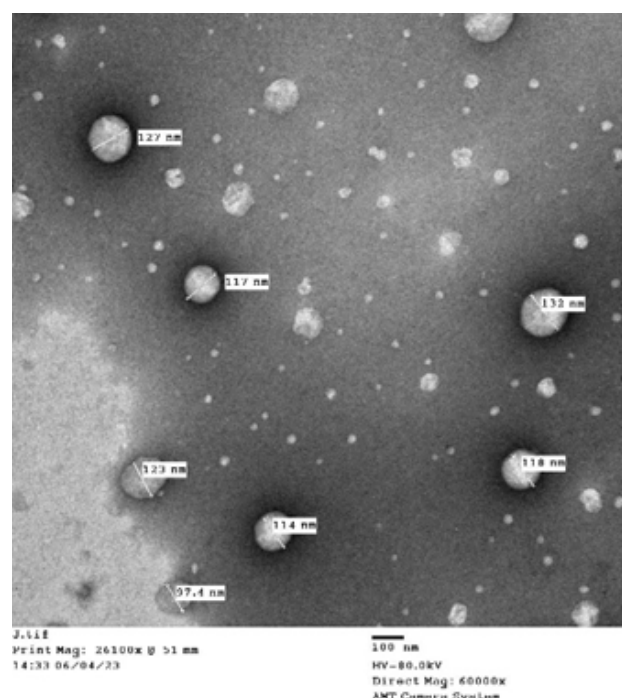


**Fig. 1:** An electron photomicrograph showing different diameters of exosomes. TEM x60000

Mice of subgroups IC and IIC were injected via tail vein with a single intravenous dose of exosomes taken from the conditioned media of one million MSCs suspended in PBS<sup>[1]</sup>.

#### Animals

The study was conducted on 47 male adult mice weighing between 20 and 50 grams on average. The Medical Research Center of the Faculty of Medicine at Ain Shams University (MASRI) is where the animals were bought and kept. Forty-two mice were kept in hygienic plastic cages covered with mesh wire. Throughout the trial, they were provided with unlimited accessibility to tap water and a typical chow diet. They were maintained with the ideal environment of light, temperature, and humidity. In addition, five mice were used for isolation of BMSCs and extraction of exosomes. This study complied with the ARRIVE Guidelines, adhered to institutional ethical guidelines for animal care. It was approved by the Ethical Committee of the Faculty of Medicine Ain Shams University with IRB approval No. FMASU MD 196/2021.

#### Experimental Design

Mice were acclimatized for 7 days and then were divided

randomly into control and cuprizone-treated groups. Each group had three subgroups (each with 7 mice).

**Group I (Control):** Mice received 1ml of distilled water orally every day for 8 weeks.

- Subgroup IA: (7 mice): Mice were sacrificed after eight weeks.
- Subgroup IB: (7 mice): Mice were given a single intravenous injection of phosphate buffer solution (PBS) through the tail vein 24 hours following the final distilled water dosage, and sacrificed four weeks later
- Subgroup IC: (7 mice): Mice were given a single intravenous injection of exosomes<sup>[1]</sup> through the tail vein 24 hours following the final distilled water dosage, and sacrificed four weeks later.

**Group II (Cuprizone-treated):** Mice were given 400 mg/kg/day of cuprizone suspended in 1ml of distilled water orally every day for 8 weeks<sup>[9]</sup>. Following that, they were randomly divided into 3 subgroups equally.

- Subgroup IIA (Cuprizone): 24 hours following the final dosage of cuprizone suspension, mice were sacrificed (after 8 weeks)
- Subgroup IIB (Recovery): 4 weeks following the final dosage of cuprizone suspension, mice were allowed to recover spontaneously without any treatment before being sacrificed.
- Subgroup IIC (exosomes treated): A single intravenous injection of exosomes was given to the mice through the tail vein 24 hours following the final dosage of cuprizone suspension. 4 weeks later, the mice were sacrificed<sup>[1]</sup>.

## Methods

### Weight measurements

The weight of each mouse was measured weekly from the start of the experiment and just before the time of sacrifice. The measured animals' weights were expressed as mean  $\pm$  SD and were subjected to statistical analysis.

### Tissue Preparation and light microscopic studies

Following ether inhalation, the animals were sacrificed by cervical dislocation at the end of the experiment (after 8 and 12 weeks). The brain was gently removed from all animals and was divided into halves by a coronal section. The brain was fixed in 10% formalin solution for one week followed by dehydration, clearing, and impregnation in soft paraffin followed by paraffin blocks embedding. Serial coronal sections were cut at 5-7  $\mu$ m thickness and were stained with Hematoxylin and Eosin stain (H&E). Luxol fast blue (LFB) for myelin staining<sup>[13]</sup>. Immunohistochemical staining was also done using polyclonal rabbit anti-mouse glial fibrillary acidic protein (GFAP) -ready to use- primary antibody and Goat anti-rabbit -ready to use- secondary antibody to detect astrocytes<sup>[14]</sup>. Rabbit anti-ionized

calcium-binding adaptor molecule 1 (Iba1) polyclonal -ready to use- primary antibody and anti-rabbit IgG -ready to use- secondary antibody (AlexaFluor®488) was used to detect microglia<sup>[14,15]</sup>. Immune sections were counterstained with hematoxylin. Brown cytoplasmic staining indicated positive GFAP and Iba-1 immune reaction. To identify any cross-reaction, negative control sections were processed by substituting phosphate buffer saline for the primary antibody. All subsequent procedures were then carried out in the same way.

### Semithin sections preparation

Very small specimens (1 mm<sup>3</sup>) from the corpus callosum's body were taken and prepared to create semithin sections for analysis under a light microscope<sup>[16]</sup>.

### Histomorphometric study

The following measurements were assessed in five distinct, non-overlapping fields from each animal's corpus callosum.

Measurements were made using Image J software (National Institutes of Health and the Laboratory for Optical and Computational Instrumentation (LOCI, University of Wisconsin).

The following parameters were measured:

1. Mean surface area of the corpus callosum in sections stained by H&E (x40)
2. Mean color density of myelin sheath surrounding nerve fibers in LFB stained sections (x40)
3. Mean number of GFAP positive astrocytes (x40),
4. Mean number of Iba1 positive microglia (x40)
5. Mean area percentage of myelinated nerve fibers in semithin sections stained by toluidine blue.

### Statistical Analysis

All the obtained morphometrical information was statistically examined. IBM SPSS statistics program version 21 (IBM Inc., Chicago, Illinois, USA) was used to calculate mean value and standard deviation (SD) of measurements obtained; from 5 fields/slide for 5 slides/mice. Means were compared by ANOVA with post-hoc test. Values were displayed in this study as mean  $\pm$  SD. The significance was established by probability of chance (*P-value*) as *p*<0.05 was regarded as statistically significant and *p*>0.05 was regarded as non-significant.

## RESULTS

### General observations

No deaths were recorded among animals in the different subgroups.

### Weight measurements

Statistical evaluation of animal weights mean values after 8 weeks from starting the experiment revealed a

significant decrease in subgroup IIA (Cuprizone) compared to control subgroups (Figure 5A). while the mean weight of mice after 12 weeks revealed a significant increase in subgroups IB & IC (control) and subgroup IIC (exosomes treated) in comparison to subgroup IIB (Recovery). Moreover, subgroup IIC showed a significant decrease compared to subgroup IB and subgroup IC (Figure 5B).

### **Histological and histo-morphometric results**

Examination of the corpus callosum from all control subgroups (IA, IB, IC) showed almost similar results in all measured parameters, and the results were expressed as control group.

#### **H&E-stained sections**

Examination of sections of the corpus callosum of mice in the control group (Group I) under a microscope revealed parallel regular closely packed myelinated nerve fibers. Oligodendrocytes were seen in between nerve fibers having rounded deeply stained nuclei surrounded by a clear rim of unstained cytoplasm. Astrocytes had little cytoplasm and more elongated pale nuclei compared to that of oligodendrocytes (Figures 2 A,A1). On the contrary, cuprizone subgroup (IIA) revealed lack of normal histological pattern of corpus callosum appeared as irregular widely separated nerve fibers, congested blood capillaries, and an apparent decreased thickness of corpus callosum in comparison to the control group (Figure 2B). In addition to the appearance of many vacuolated areas in between nerve fibers with frequent areas of disrupted nerve fibers were seen (Figures 2 B,B1). Eccentric pyknotic nuclei of oligodendrocytes were also observed (Figure 2B). The recovery subgroup (IIB) showed partial improvement, histological damage was represented by the presence of numerous vacuoles, eccentric pyknotic nuclei and areas of disrupted nerve fibers (Figures 2 C,C1). Notable improvement was observed after treatment with BMSCs derived exosomes (subgroup IIC) where the most of the oligodendrocytes and nerve fibers appeared normal, and the corpus callosum showed a moderate improvement. Few oligodendrocytes were occasionally seen with deeply stained nuclei. Also, there were several cells between the nerve fibers with large vesicular nuclei (Figures 2 D,D1).

The smallest mean surface area of the corpus callosum in H&E sections was measured in subgroup IIA (cuprizone). This value revealed a significant decline in comparison to control group and exosomes treated subgroup IIC. While exosomes treated subgroup IIC revealed a significant increase in the mean surface area in comparison to cuprizone IIA and recovery IIB subgroups and a significant decline was noticed in comparison to control group (Figure 2E).

#### **LFB-stained sections**

Sections of the corpus callosum stained by luxol fast blue (LFB) in the control group and exosomes treated subgroup showed dense blue stained parallel, regular closely packed myelinated nerve fibers. In cuprizone and

recovery subgroups, pale blue-stained widely separated nerve fibers were seen. The smallest mean optical density of myelin sheath in LFB-stained sections was measured in subgroup IIA (cuprizone). This value revealed a significant decline compared to control group and subgroup IIC (exosomes treated). While subgroup IIC revealed a significant increase in comparison to subgroup IIA and subgroup IIB (Figures 3 A-E).

#### **Immunohistochemical results**

GFAP immunohistochemical stained sections of the corpus callosum of the control and exosomes treated subgroups revealed few hypertrophic GFAP-positive astrocytes. In cuprizone and recovery subgroups, many hypertrophic GFAP-positive astrocytes were seen. The highest number for GFAP-positive astrocytes was measured in subgroup IIA (cuprizone). This value revealed a significant increase in comparison to all other subgroups. In addition, subgroup IIC revealed a significant decline in comparison to subgroup IIA and subgroup IIB as well as a significant increase in comparison to control group (Figures 4 A-E).

Examination of Iba1 immunohistochemical stained sections of the corpus callosum in control group and exosomes treated subgroup revealed few microglia with Iba1 positive reactions. In cuprizone & recovery subgroups, many microglia with Iba1-positive reactions and hypertrophic cellular bodies were seen. The highest number of Iba1 positive microglia was measured in subgroup IIA (cuprizone). This value revealed a significant increase in comparison to control subgroups and subgroup IIC (exosomes treated). Subgroup IIC revealed a significant decline in comparison to subgroup IIA and subgroup IIB and a significant increase in comparison to control group (Figures 4 A1- E1).

#### **Results of Toluidine blue stained semithin sections**

Semi-thin sections of the control group's corpus callosum stained with toluidine blue revealed fasciculi of myelinated nerve fibers. Between the nerve fasciculi, glial cells were visible. Cuprizone & recovery subgroups showed extensively demyelinated nerve fibers with few areas of myelinated nerve fibers. While in exosomes treated subgroup, an apparent increased number of myelinated nerve fibers was seen with few scattered areas of demyelinated nerve fibers. The smallest mean area percentage of myelinated nerve fibers was measured in subgroup IIA (cuprizone).

In comparison to control group and subgroup IIC (exosomes treated), this value revealed a significant decline. While, subgroup IIC demonstrated a significant decline when compared to control group and a significant increase when compared to subgroups IIA and IIB (Figures 4 A2- E2).



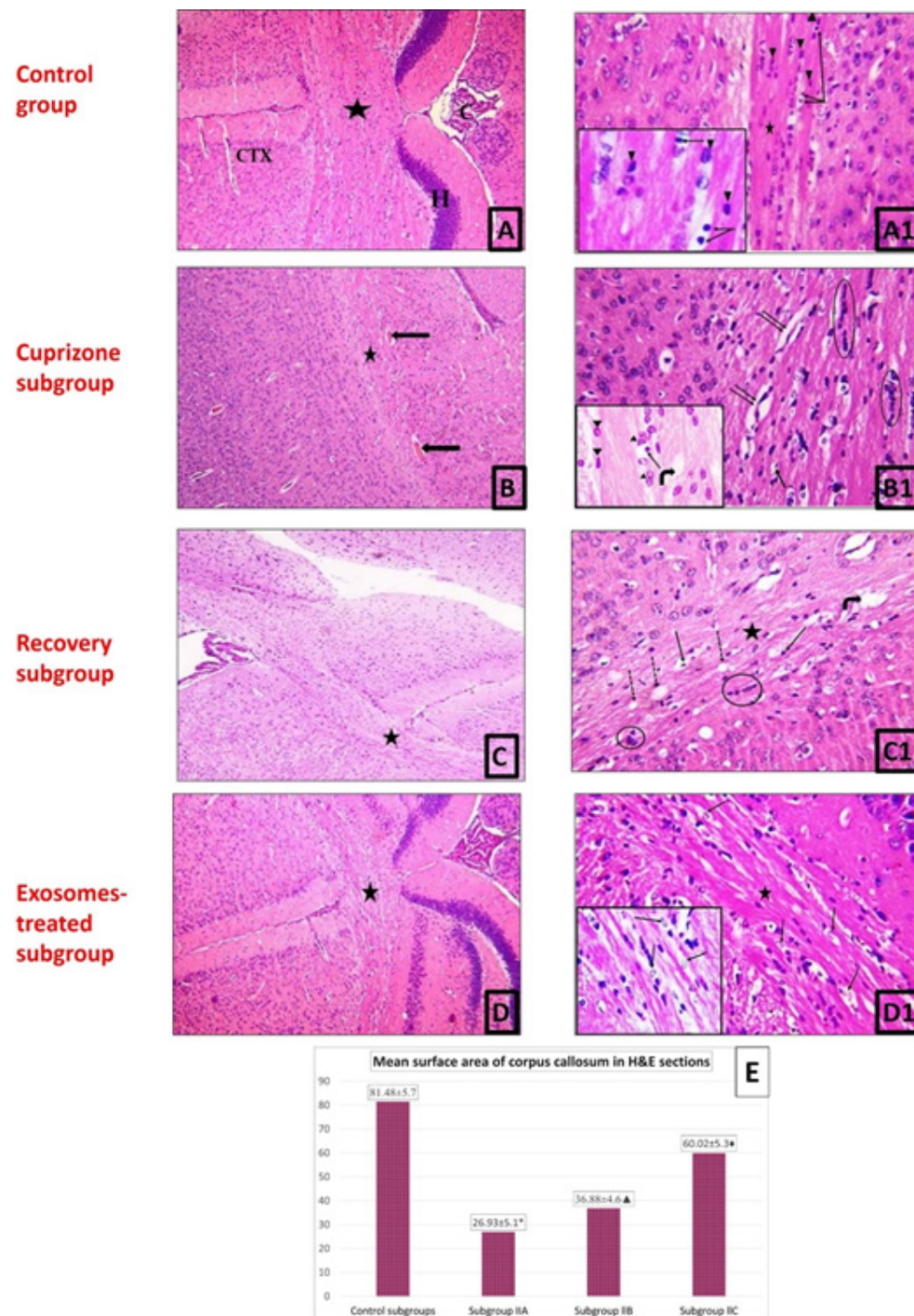


**Fig. 2:** Photomicrographs of H&E coronal sections of the brain (magnifications: low x100, high x400, insets x1000). Control group (A, A1) showing the corpus callosum formed of many nerve fibers (◆), oligodendrocytes having rounded deeply stained nuclei surrounded by a clear rim of unstained cytoplasm (↑), astrocytes with elongated pale nuclei (▲); C: choroid plexus of 3rd ventricle; CTX: cerebral cortex; H: hippocampus. Cuprizone subgroup (B, B1) showing an apparent decreased thickness of corpus callosum (◆) with congestion of the blood capillaries (thick arrows), eccentric pyknotic nuclei of oligodendrocyte (↑), vacuolated areas (↑↑), area of disrupted nerve fibers (bent arrow), mononuclear cellular infiltration (black oval), and many vesicular nuclei of astrocytes (▲). Recovery subgroup (C, C1) showing pale stained nerve fibers of corpus callosum (◆) with many vacuoles (dash arrows), area of disrupted nerve fibers (bent arrow), eccentric pyknotic nuclei of oligodendrocytes (↑) and mononuclear cellular infiltration (black circles). Exosome-treated subgroup (D, D1) showing corpus callosum formed of some deeply stained nerve fibers while others are moderately stained (◆), multiple vesicular nuclei in between nerve fibers (↑). [E] Histogram showing the mean surface area of corpus callosum (±SD) in H&E-stained sections in different experimental subgroups. (\*) Significant to control subgroups and subgroup IIC, (◆) Significant to control subgroups, subgroups IIA and IIB; (▲) Significant to control subgroups and subgroup IIC.

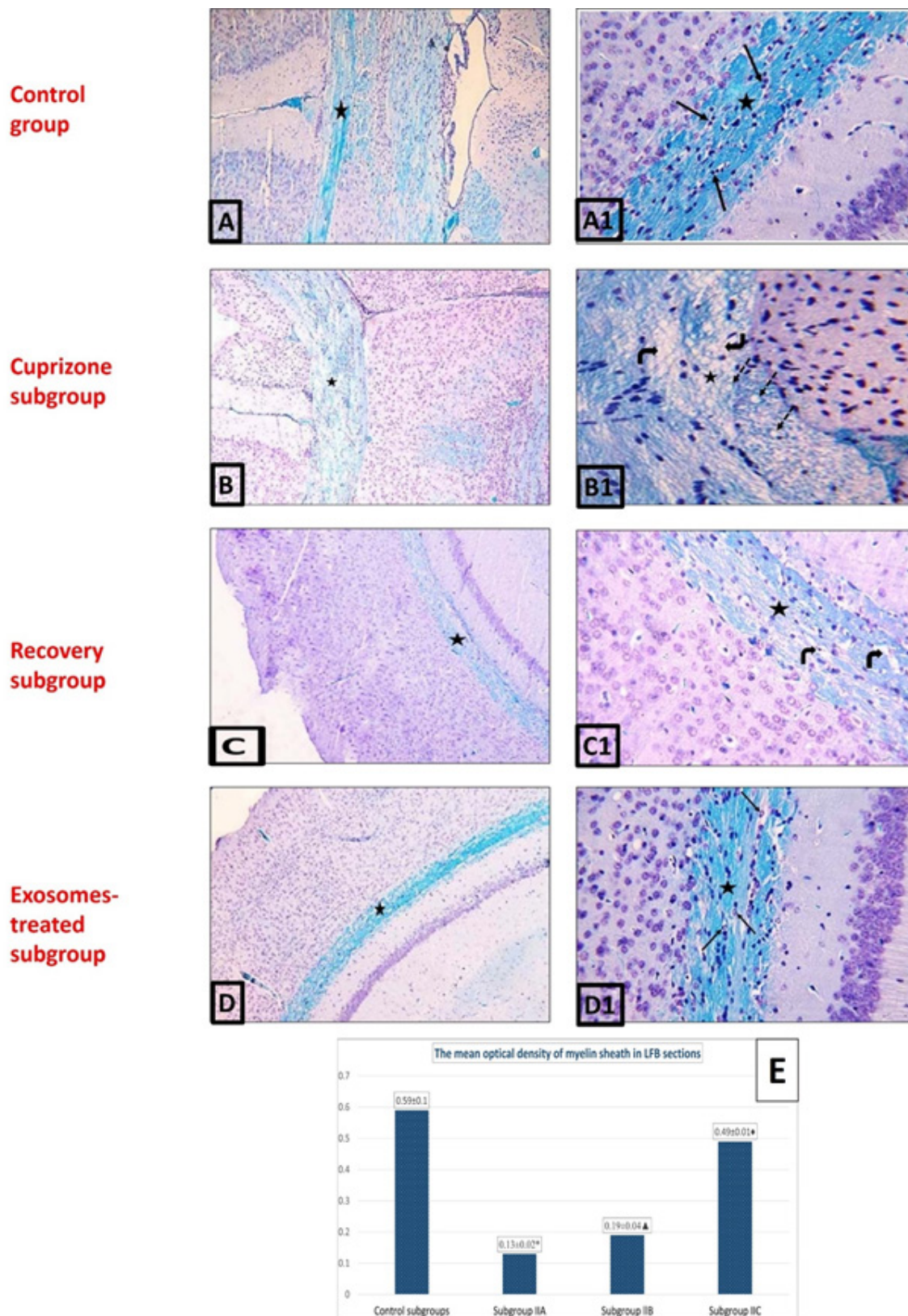


**Fig. 3:** Photomicrographs of LFB stained sections of the corpus callosum (magnification: low x100 and high x400). Control group (A, A1) and exosomes treated subgroup (D, D1) showing dense blue stained myelinated nerve fibers (♦), many vesicular nuclei (†). Cuprizone subgroup (B, B1) and recovery subgroup (C, C1) Showing pale blue stained nerve fibers (♦), many vacuoles (dash arrows), areas of disrupted nerve fibers (bent arrows). [E] Histogram showing the mean optical density (±SD) of myelin sheath in the corpus callosum in LFB-stained sections in different experimental subgroups. (\*) Significant compared to control subgroups and subgroup IIC; (▲) Significant compared to control subgroups and subgroup IIC; (♦) Significant compared to subgroup IIA and subgroup IIB.



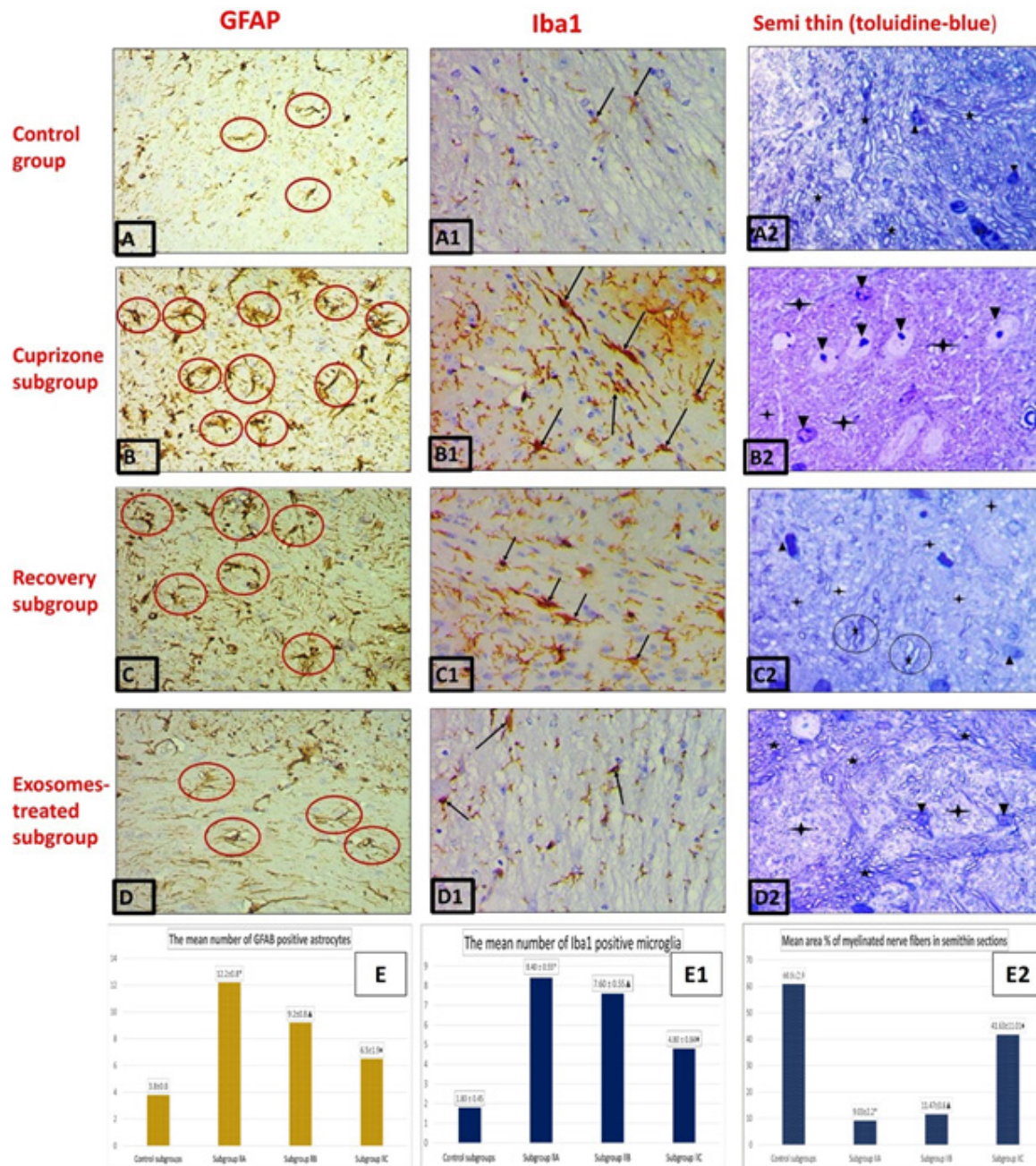


**Fig. 4:** [A-D] GFAP immune stained sections: showing GFAP positive astrocytes (red circles). Notice few thin processes in control group. An apparent increased number of hypertrophic astrocytes and multiple prominent cellular processes are seen in cuprizone and recovery subgroups. An apparent decreased number and processes of astrocytes are seen in exosomes group. [A1-D1] Iba-1 immune stained sections: showing microglia with Iba-1 positive reactions (†). Notice few number in control group. An apparent increased number of microglia with hypertrophic cellular bodies and processes are seen in cuprizone and recovery subgroups. Exosome treated subgroup shows an apparent decrease in number of microglia. [A2-D2] semi-thin section of corpus callosum of control group (A2) showing many myelinated nerve fibers arranged in groups (♦), glial cells are seen in between the nerve groups (▲), patent blood vessel (BV). Cuprizone subgroup (B2) showing extensively demyelinated nerve fibers of corpus callosum (♦) and many glial cells are observed in between nerve fasciculi (▲). Recovery subgroup (C2) showing apparent increase in number of demyelinated nerve fibers of corpus callosum (♦) with scattered glial cells (▲) with few areas of myelinated nerve fibers (♦). Exosomes treated subgroup (D2) showing apparent increase in number of myelinated nerve fibers arranged in groups (♦). Glial cells are also observed in between nerve fasciculi (▲) with the presence of areas of demyelination (♦). Histograms Showing the mean (±SD) of: [E] number of GFAP positive astrocytes in the corpus callosum in different subgroups; [E1] number of Iba-1 positive microglia in the corpus callosum in different subgroups; [E2] area percentage of myelinated nerve fibers in the corpus callosum in semithin sections in different subgroups. (\*) Significant compared to control subgroups and subgroup IIC; (▲) Significant compared to control subgroups and subgroup IIC; (♦) Significant compared to subgroup IIA and subgroup IIB.

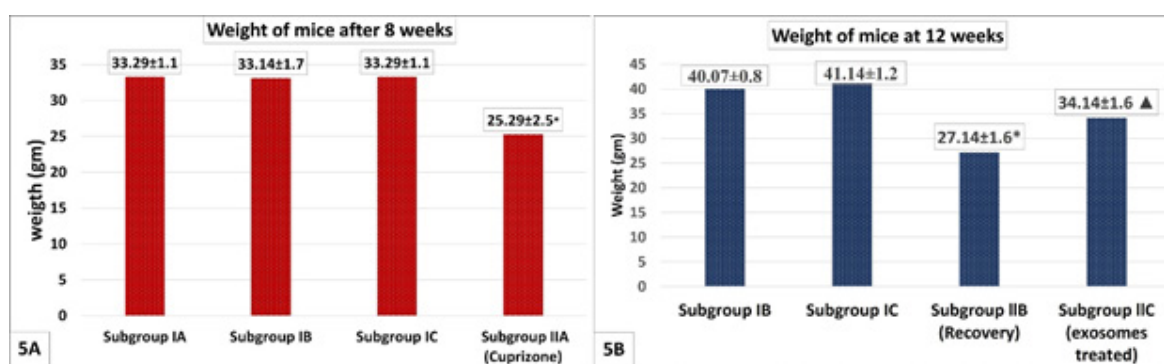


**Fig. 5:** Showing the mean weight (gm) (±SD) of mice in different experimental subgroups. [A] after 8 weeks from the beginning of experiment; (\*) Significant compared to control subgroups. [B] after 12 weeks, (\*) Significant from subgroups IB, IC and IIC; (▲) Significant from subgroups IB, IC and IIB.

## DISCUSSION

Multiple sclerosis (MS) is a persistent demyelinating illness of the central nervous system<sup>[2]</sup>. Axonal injury and the degradation of myelin sheaths are its defining features<sup>[4]</sup>. The current study was to determine whether exosomes generated from BMSCs may have an impact on the structure of the mice's corpus callosum in an experimental cuprizone model of multiple MS.

A copper-chelating substance called cuprizone is given orally to rodents<sup>[17]</sup>. It was used in the current study for induction of MS. Cuprizone is an experimental toxic animal model of demyelination. It induced demyelination of CNS, mainly in the corpus callosum by encouraging mature oligodendrocytes (myelin-forming cells) to undergo apoptosis<sup>[3,18]</sup>. In addition to hypertrophy or proliferation of glial cells including astrocytes and microglial cells (astrogliosis and microgliosis)<sup>[4,19]</sup>.

Although the frequency of MS has increased all over the world, no remyelination therapy is available and still there are very few available therapeutic approaches for MS treatment. Accordingly, alternative strategies must be tested and there is an urgent need for novel therapeutic approaches. One of the valuable strategies in the treatment of MS is the use of exosomes which are involved in the remyelination process by increasing oligodendrocytes activity<sup>[6]</sup>. In addition, exosomes act as a communicating vehicle, between neurons and glial cells. Furthermore, exosomes serve as biological information carriers. (e.g., miRNA, mRNA, and protein) to distant cells<sup>[20,21]</sup>. Exosomes, cell-free therapy had many advantages over MSCs itself such as reduced immunogenicity because MHC-II is absent and MHC-I expression is low<sup>[22]</sup>.

In the current study the statistical analysis of animal weights after 8 weeks revealed a significant decline in cuprizone subgroup IIA in comparison to the control group. Similar results were observed by many authors<sup>[9,23,24]</sup>. The weight loss following cuprizone ingestion was attributed to decrease in the food consumption due to its systemic harmful effects on the body as reported previously by Steelman *et al.*<sup>[25]</sup>. On the other hand, performing statistical analysis on the previous parameter at the end of the

experiment (after 12 weeks) showed a significant increase in weight in exosomes treated subgroup IIC compared to recovery subgroup IIB. This might be explained by gradual weight gain with increased food consumption due to the discontinuation of cuprizone and the effect of exosomes administration.

In the current work, examination of H&E-stained sections of the corpus callosum in mice of cuprizone (IIA) & recovery (IIB) subgroups revealed vacuolated areas in-between nerve fibers and focal areas of disrupted nerve fibers. Examination of the semi-thin sections of corpus callosum confirmed the previous findings. It showed extensive demyelination of nerve fibers. This was statistically confirmed by measuring the mean area percentage of myelinated nerve fibers. In subgroup IIA, these findings might be explained by oligodendrocytes apoptosis with subsequent demyelination and disrupted nerve fibers as reported by Barkat *et al.*<sup>[24]</sup>. Furthermore, other authors reported the appearance of vacuoles. Joost *et al.*<sup>[26]</sup> attributed the previous finding to myelin detachments with partial contact with the axon. In subgroup IIB, these results might be explained by the decrease in remyelination capacity with time due to poor migration of oligodendrocytes precursor cells (OPCs) and inability to differentiate to oligodendrocytes, which was consistent with the findings of Gingele *et al.*<sup>[27]</sup>, who found that after feeding mice 0.4% cuprizone for 6.5 weeks, the corpus callosum completely demyelinated. Additionally, there is a significant buildup of microglia and a nearly complete loss of mature oligodendrocytes. They also mentioned that although remyelination was started, it was not finished.

Zhang *et al.*<sup>[28]</sup> stated that OPCs differentiated into oligodendrocytes to preserve myelin regeneration in diseases affecting the central nervous system. Otherwise, MS and other chronic inflammatory demyelinating diseases were not efficiently treated by endogenous remyelination. It was added that chronic cuprizone intoxication was followed by incomplete remyelination with a significant slow myelin repair as well as disturbed endogenous regenerative process<sup>[2]</sup>. Demyelinated areas were continuously remyelinated in the early stages of the disease, but as the condition worsened, this process



lost effectiveness. Furthermore, delayed and ineffective remyelination with lack of regeneration of damaged tissue had occurred in parts of the brain that had persistent demyelination at advanced stages of the disease. Ineffective OPCs stimulation and the incapacity to develop into mature myelinating cells were the causes of this failure<sup>[29]</sup>.

In subgroup IIC, H&E-stained sections, most of the corpus callosum was composed of regular nerve fibers with partial restoration of its histological structure in comparison to that of the cuprizone group IIA. Examination of the semi-thin sections confirmed the previous findings. It showed an apparent increase in myelinated nerve fibers which were arranged in fasciculi or groups with focal areas of demyelination. This finding was statistically confirmed by measuring the mean area percentage of myelinated nerve fibers. These findings might be explained by the dual impact of both discontinuations of cuprizone and exosomes administration, which were in accordance with the findings of Gharib *et al.*<sup>[30]</sup> who investigated how an intraperitoneal injection of MSC microvesicles (0.2 mg/kg body weight) affected a model of multiple sclerosis in mice. They observed an apparent improvement, where the nerve fibers looked normal with a slight vacuolation in-between. These semithin findings also agreed with those of Barkat *et al.*<sup>[24]</sup>. In addition, in the current study, glial cells were less encountered in subgroup IIC than in subgroup IIA. Similarly, Alatrash *et al.*<sup>[31]</sup> also reported that adipose-derived MSCs (ADMSCs) and ADMSC-derived MVs significantly reduced the glial cells number in experimental autoimmune encephalomyelitis, a model of multiple sclerosis.

Some authors suggested that the beneficial consequences of MSC-exosomes therapy in MS had mainly concentrated on its immunomodulatory characteristics, in addition to its pro-inflammatory regulator role that led to reduction of neuroinflammation with subsequent reduction of demyelination and promoting CNS recovery<sup>[32]</sup>. Furthermore, BMSCs-derived exosomes had the ability to cross BBB and reach the brain and target cells directly to induce enhancement of remyelination, neuro-regeneration and enhance the recovery of neurological and cognitive functions following demyelination in animal models<sup>[20]</sup>. They added that exosomes stimulate OPCs differentiation into mature oligodendrocytes and remyelination, reducing axonal damage, and regulating microglial cells M1/M2 polarization.

Cuprizone's harmful effect on oligodendrocytes was achieved by the recruited microglia and astrocytes releasing proapoptotic cytokines like interferon-gamma (INF- $\gamma$ ) and tumor necrosis factor-alpha (TNF- $\alpha$ ). The disruption of intracellular copper levels caused by these cytokines ultimately results in myelin breakdown and oligodendrocyte death<sup>[33]</sup>.

In H&E-stained sections, mononuclear cellular infiltrations were also noticed in subgroups IIA&IIB. This agreed with Wolf *et al.*<sup>[34]</sup> who stated that it was thought

that T- and B-cells, in particular, played a minority role during cuprizone-induced demyelination, despite the fact that the MS model had reported mild BBB disruption.

In current study, H&E-stained sections of subgroup IIC, There were several cells with vesicular nuclei between the nerve fibers which might be explained by activation and recruitment of OPCs and oligodendrocytes to restore myelin sheath. In support of this finding, it was reported that in response to myelin injury, OPCs gained a reactive phenotype with subsequent proliferating and migrating to the injury site and eventually differentiating into mature myelinated oligodendrocytes<sup>[29]</sup>. Moreover, it was previously suggested that new OPCs could be originated from parenchyma of the corpus callosum and the subventricular zones<sup>[2]</sup>.

In current work, corpus callosum sections of mice in subgroups IIA and IIB stained with LFB revealed demyelinated nerve fibers that were pale blue in color. Also, many vacuoles and areas of disrupted nerve fibers were noticed. These findings could be explained by the demyelination of nerve fibers due to apoptosis of oligodendrocytes. While, subgroup IIC, it showed dense blue stained nerve fibers comparable to that of subgroup IIA. This result might be explained by partial restoration of the normal histological structure of the corpus callosum with myelinated nerve fibers. This observation was statistically confirmed by measuring the mean optical density of LFB staining. Similarly, Kipp *et al.*<sup>[35]</sup> studied acute and chronic toxic model of MS induced by cuprizone in mice and found a decrease in the mean optical density of LFB staining. They explained their findings by oligodendrocyte degradation instead of an actual assault on the myelin sheath. The effect of oral cuprizone was also studied in rats at different times after 4, 5, 6, and 7 weeks. The demyelinated or hypomyelinated areas were stained pale by LFB<sup>[36]</sup>. In subgroup IIB, these findings might be explained by incomplete remyelination following cessation of cuprizone in case of chronic demyelination, similar finding was detected by Li *et al.*<sup>[37]</sup>.

In the present study, corpus callosum immuno-histochemical staining sections for GFAP in cuprizone subgroup IIA revealed a significant increase in number of GFAP positive hypertrophic astrocytes with multiple prominent cellular processes. This finding agreed with the results of previous studies who attributed it to reactive astrocytosis following cuprizone ingestion<sup>[27,28,38]</sup>. As soon as astrocytes were stimulated, they increased GFAP expression and many cells were apparent<sup>[2]</sup>.

In recovery subgroup IIB, the mean number of GFAP-positive astrocytes was significantly increased compared to control group and subgroup IIC and significantly decreased compared to subgroup IIA. This result was in accordance with the findings of Sachs *et al.*<sup>[39]</sup>. Furthermore, it was stated that GFAP expression levels decline again when cuprizone intoxication stops, but they are still higher than in control mice, suggesting that astrocyte activation

during remyelination is still occurring<sup>[40]</sup>. The processes of demyelination and remyelination were significantly influenced by the astrocytes. After cuprizone intoxication, they proliferate, and microglia are subsequently activated and recruited<sup>[41]</sup>. Moreover, A1 and/or A2 are two different phenotypes of reactive astrocytes that may form during neuroinflammation. The A1 was highly neurotoxic and contributed to neuroinflammation associated with demyelination. On the other hand, A2 astrocytes had neuroprotective and anti-inflammatory properties contributing to the remyelination process<sup>[29]</sup>. While subgroup IIC showed a significant decrease in the number of GFAP-positive hypertrophic astrocytes in comparison to subgroups IIA&IIB and a significant increase in comparison to control group. This finding was consistent with those of Zhan *et al.*<sup>[2]</sup> who reported that anti-GFAP antibodies exclusively identified active astrocytes, not all of them.

In the current study, corpus callosum immuno-histochemical staining sections for Iba1 in cuprizone subgroup IIA & recovery subgroup IIB revealed a significant increase in the number of microglia with Iba1 positive reactions with hypertrophic cellular bodies and processes compared to control subgroups and subgroup IIC. Similar results were explained by reactive microgliosis following cuprizone ingestion as stated by Zhang *et al.*<sup>[28]</sup> and Kipp *et al.*<sup>[42]</sup>. Moreover, the whole cell body as well as the tiny, distal processes of microglia are marked by anti-Iba1 antibodies as either activated or not. Microglia retracted their fine processes following activation, and their cell bodies and processes both appeared bigger<sup>[2]</sup>. Moreover, pro-inflammatory M1- microglia became activated during the progression of MS which had a significant role in the demyelination process. This demyelinating effect was produced by secreting many pro-inflammatory mediators including cytokines and chemokines that increased peripheral immune cell recruitment and activation, causing neuroinflammation<sup>[20]</sup>.

Regarding recovery subgroup IIB, the increased number of microglia might be explained by reactive microgliosis due to incomplete remission following cessation of cuprizone, as microglia had an important role in both demyelination and remyelination processes. A similar explanation was reported by Sach *et al.*<sup>[39]</sup> after 7 weeks' of recovery. On the other hand, Gudi *et al.*<sup>[43]</sup> claimed that in mice given cuprizone, active microglia still exist in lesions that are continuously demyelinated at a low level. While in subgroup IIC, a significant decrease in the number of Iba1-positive microglia was noticed. This could be related to anti-inflammatory potential of exosomes with subsequent decrease of inflammatory microglia. A similar finding was detected by Laso-Garcia *et al.*<sup>[1]</sup>. Microglia were activated during CNS damage and secreted IL-1, IL-12, IL-23, TNF $\alpha$ , and inducible nitric oxidase synthase (pro-inflammatory M1 phenotype), which could enhance inflammation and cytotoxicity. On the other hand, by secreting transforming growth factor beta (TGF $\beta$ ), IL-4, IL-

10, and IL-13, the anti-inflammatory M2-phenotype may contribute to neuroprotection and decrease inflammation. Microglia promoted remyelination by removing myelin debris that was essential for the start of this process. After that, they released substances that encouraged OPCs to migrate, proliferate, and develop into fully developed myelinating oligodendrocytes<sup>[44]</sup>.

---

## CONCLUSION

In the cuprizone model of MS, single injection of bone marrow mesenchymal stem cells derived exosomes were demonstrated to improve demyelination of mice's corpus callosum. Therefore, exosomes may offer a novel approach to MS therapy.

---

## ETHICS APPROVALS

All animal care and methods were in consistent with institutional guidelines for animal care and use, published by the National Institutes of Health. In addition, the institutional Animals Care and Use Committee (ACUC) and Research Ethics Committee (FMASUS REC) approved the experimental protocol with Federal wide assurance No. 000175. 85 (IRP approval No. FMASU MD 196/2021.).

---

## AUTHOR CONTRIBUTIONS

The authors confirm contributions to the paper as follows: B.A.A.H, N.M.ES, G.A.H and M.H.R.A study conceptualization, design, and Validation; B.A.A.H, data collection, Formal analysis, Investigation, Resources, Writing the Original Draft. N.M.ES, G.A.H and M.H.R.A Supervision, analysis, Review & Editing; and interpretation of results. All authors reviewed the results and approved the final version of the manuscript.

---

## CONFLICT OF INTERESTS

There are no conflicts of interest.

---

## REFERENCES

1. Laso-Garcia F, Ramos-Cejudo J, Carrillo- Salinas FJ, Otero-Ortega L, Feliu A, Gomez-de Frutos M, *et al.*(2018): Therapeutic Potential of Extracellular Vesicles Derived from Human Mesenchymal Stem Cells in a Model of Progressive Multiple Sclerosis. *PLoS One*. 13(9):1-16. e0202590. doi: 10.1371/journal. Pone.0202590
2. Zhan J, Mann T, Joost S, Behrangi N, Frank M, Kipp M (2020): The Cuprizone Model: Dos and Do Nots. *Cells*. 9, 843: 1-21. doi: 10.3390/cells9040843
3. Be'nardais K, Kotsiari A, kuljec JS, Koutsoudaki PN, Gudi V, Singh V, Vulinovic F, Skripuletz T, Stangel M (2013): Cuprizone [Bis(Cyclohexylidenehydrazide)] is Selectively Toxic for Mature Oligodendrocytes. *Neurotox Res*. 24: 244-250. doi: 10.1007/s12640-013-9380-9

4. Mojaverrostami S, Pasbakhsh P, Madadi S, Nekoonam S, Zarini D, Noori L, Shiri E, Salama M, Zibara K, Kashani IR (2020): Calorie Restriction Promotes Remyelination in a Cuprizone-Induced Demyelination Mouse Model of Multiple Sclerosis. *Metabolic Brain Disease*. 35:1211–1224. doi: /10.1007/s11011-020-00597-0
5. Konala VB, Mamidi MK, Bhonde R, Das AK, Pochampally R, Pal R (2016): The Current Landscape of the Mesenchymal Stromal Cell Secretome: A New Paradigm for Cell-Free Regeneration. *Cytotherapy*. 18(1): 13–24. doi:10.1016/j.jcyt.2015.10.008
6. Osorio-Querejeta I, Alberro A, Muñoz-Culla M, Mäger I, Otaegui D (2018): Therapeutic Potential of Extracellular Vesicles for Demyelinating Diseases; Challenges and Opportunities. *Front. Mol. Neurosci*. 11: 1-8. doi: 10.3389/fnmol.2018.00434
7. Miao C, Wang X, Zhou W, Huang J (2021): The Emerging Roles Of Exosomes In Autoimmune Diseases, With Special Emphasis On MicroRNAs In Exosomes. *Elsevier* 169. doi: 10.1016/j.phrs.2021.105680
8. Otero- Ortega L, GoÁmez de Frutos MC, Laso-García F, Rodríguez-Frutos B, Medina-Gutiérrez E, López JA, *et al.*, (2018): Exosomes Promote Restoration After An Experimental Animal Model Of Intracerebral Hemorrhage. *J Cereb Blood Flow Metab*. 38:767±779. doi: 10.1177/0271678X17708917
9. Zhen W, Liu A, Lu J, Zhang W, Tattersall D, Wang J (2017): An Alternative Cuprizone-Induced Demyelination and Remyelination Mouse Model. *ASN Neuro*. 1-9. doi: 10.1177/1759091417725174
10. Zhang J, Guan J, Niu X, Hu G, Guo S, Li Q, Xie Z, Zhang C, Wang Y (2015): Exosomes Released from Human Induced Pluripotent Stem cells-Derived MSCs Facilitate Cutaneous Wound Healing by Promoting Collagen Synthesis and Angiogenesis. *Journal of translational medicine*. 13(1):1-4. doi: 10.1186/s12967-015-0417-0
11. Lane, R.E., Korbie, D., Trau, M., Hill, M.M. (2017): Purification Protocols for Extracellular Vesicles. In: Kuo, W., Jia, S. (eds) *Extracellular Vesicles. Methods in Molecular Biology*, vol 1660. Humana Press, New York, NY doi: 10.1007/978-1-4939-7253-1\_10
12. Petersen KE, Manangon E, Hood JL, Wickline SA, Fernandez DP, Johnson WP, Gale BK (2014): A Review of Exosome Separation Techniques and Characterization of B16-F10 Mouse Melanoma Exosomes with AF4-UV-MALS-DLS-TEM. *Anal Bioanal Chem* 406, 7855–7866. doi: 10.1007/s00216-014-8040-0
13. Highley J R, Sullivan N (2019): Neuropathology and muscle biopsy techniques. In: *Bancroft's Theory and Practice of Histological Techniques*. Suvarna SK, Layton C, Bancroft JD (Eds.), 8th edition, Churchill Livingstone Elsevier; PP.:311-312.
14. Sanderson T, Wild G, Cull AM, Marston G, Zardin G (2019): Immunohistochemical and Immunofluorescent Techniques. In: *Bancroft's Theory and Practice of Histological Techniques*. Suvarna SK, Layton C, Bancroft JD (Eds.), 8th edition, Churchill Livingstone Elsevier; pp.: 377-394.
15. Klein B, Mrowetz H, Barker CM, Lange S, Rivera FJ, Aigner L (2018): Age Influences Microglial Activation after Cuprizone-Induced Demyelination. *Front. Aging Neurosci*. 10:278. doi: 10.3389/fnagi.2018.00278
16. Woods AE, Stirling JW (2013): Transmission Electron Microscopy. In: *Bancroft's Theory and Practice of Histological Techniques*. Suvarna SK, Lyton C and Bancroft JD (Eds.), 7th edition, Churchill Livingstone Elsevier; pp.: 493-538.
17. Toomey LM, Papini M, Lins B, Wright AJ, Warnock A, McGonigle T, Hellewell SC, Bartlett CA, Anyaegbu C, Fitzgerald M (2021): Cuprizone Feed Formulation Influences the Extent of Demyelinating Disease Pathology. *Sci Rep* 11, 22594 . doi:10.1038/s41598-021-01963-3
18. Procaccini C, De Rosa V, Pucino V, Luigi Formisano L, Matarese G (2015): Animal Models of Multiple Sclerosis. *Eur J Pharmacol*. 759: 182–191. doi:10.1016/j.ejphar.2015.03.042
19. Kipp M (2020): Oligodendrocyte Physiology and Pathology Function. *Cells*. 9 (9), 2078: 1-5. doi: 10.3390/cells9092078
20. Zhang J, A. Buller B, Zhang ZG, Zhang Y, Lu M, L. Rosene D, Medalla M, L. Moore T, Chopp M (2022): Exosomes Derived from Bone Marrow Mesenchymal Stromal Cells Promote Remyelination and Reduce Neuroinflammation in the Demyelinating Central Nervous System. *Experimental Neurology*. 347:113895. doi: /10.1016/j.expneurol.2021.113895
21. Palacio PL, Pleet ML, Reategui E, Magana SM (2023): Emerging Role of Extracellular Vesicles in Multiple Sclerosis: From Cellular Surrogates to Pathogenic Mediators and Beyond. *Journal of Neuroimmunology*. 377: 578064. doi: 10.1016/j.jneuroim.2023.578064
22. Allegretta C, D'Amico E, Manuti V, Avolio C, Conese M (2022): Mesenchymal Stem Cell-Derived Extracellular Vesicles and Their Therapeutic Use in Central Nervous System Demyelinating Disorders. *Int J Mol Sci*. 23(7): 3829. doi: 10.3390/ijms23073829
23. Leopold P, Schmitz C, Kipp M (2019): Animal Weight Is an Important Variable for Reliable Cuprizone-Induced Demyelination. *J Mol Neurosci* 68, 522–528. doi:10.1007/s12031-019-01312-0



24. Barkat MA, El-Agawany A, Khanfour AA, Kelada MN, Nabil I, Abdelmonsif DA, Dief AE (2020): The potential Therapeutic Effect of Adipose Tissue-derived Mesenchymal Stem Cell Transplantation on Cuprizone Model of Multiple Sclerosis in the Mice. *Scopus*. 43(1): 122-143. doi:10.21608/ejh.2019.13731.1129
25. Steelman AJ, Thompson JP, Li J (2012): Demyelination and Remyelination in Anatomically Distinct Regions of the Corpus Callosum Following Cuprizone Intoxication. *Neurosci Res*. 72(1):32-42. doi:10.1016/j.neures.2011.10.002
26. Joost S, Schweiger F, Pfeiffer F, Ertl C, Keiler J, Frank M, Kipp M (2022): Cuprizone Intoxication Results in Myelin Vacuole Formation. *Front. Cell. Neurosci*. 16: 1-9. 709596. doi: 10.3389/fncel.2022.709596
27. Gingele S, Henkel F, Heckers S, Moellenkamp TM, Hümmert MW, Skripuletz T, Stangel M, Gudi V (2020): Delayed Demyelination and Impaired Remyelination in Aged Mice in the Cuprizone Model. *Cells*. 9(9), 945:1-19. doi:10.3390/cells9040945
28. Zhang N, Liu C, Zhang R, Jin L, Yin X, Zheng X, Siebert H, Li Y, Wang Z, Loers G, Petridis AK (2020): Amelioration of Clinical Course and Demyelination in the Cuprizone Mouse Model in Relation to Ketogenic Diet. *Food Funct*. 11: 5647–5663.
29. Sidoryk-Węgrzynowicz M, Dąbrowska-Bouta B, Grzegorz Sulkowski G, Strużynska L (2021): Nanosystems and Exosomes as Future Approaches in Treating Multiple Sclerosis. *Eur J Neurosci*. 54:7377–7404. doi: 10.1111/ejn.15478
30. Gharib DM, Rashed LA, Yousuf AF, El-Shawwa MM, Saber SM, Ibrahim B MM, Kamel MM (2022): Therapeutic Effect of Microvesicles Derived From BM-MSCS Transplantation And/ Or Melatonin In Cuprizone Model of Multiple Sclerosis: A Pharmacodynamic Biochemical Assay. *Egypt. J. Chem*. 65 (10): 153 – 169. doi: 10.21608/ejchem.2022.112611.5107
31. Alatrash R, Golubenko M, Martynova E, Garanina E, Mukhamedshina y, Khaiboullina S *et al.*, (2023): Genetically Engineered Artificial Microvesicles Carrying Nerve Growth Factor Restrains the Progression of Autoimmune Encephalomyelitis in an Experimental Mouse Model. *Int J Mol Sci*. 5; 24 (9): 8332. doi: 10.3390/ijms24098332
32. Giunti D, Marini C, Parodi B, Usai C, Milanese M, Bonanno G, Kerlero de Rosbo N, Uccelli A (2021): Role of MiRNAs Shuttled by Mesenchymal Stem Cell-Derived Small Extracellular Vesicles in Modulating Neuroinflammation. *Sci. Rep.*; 11:1-16; 1740. doi: 10.1038/s41598-021-81039-4
33. Bolcskei K, Kriszta G, Saghy E, Payrits M, Sipos E, Vranesics A *et al.*, (2018): Behavioural Alterations and Morphological Changes are Attenuated by the Lack of TRPA1 Receptors in the Cuprizone-Induced Demyelination Model in Mice. *J Neuroimmunol*. 320:1-10. doi: 10.1016/j.jneuroim.2018.03.020
34. Wolf Y, Shemer A, Levy-Efrati L.; Gross M, Kim J.S, Engel A, David E, Chappell-Maor L, Grozovski J, Rotkopf R, *et al.*, (2018): Microglial MHC class II is Dispensable for Experimental Autoimmune Encephalomyelitis and Cuprizone-induced Demyelination. *Eur. J. Immunol*. 48: 1308–1318. doi: 10.1002/eji.201847540
35. Kipp M, Clarner T, Dang J, Copray S, Beyer C (2009): The Cuprizone Animal Model: New Insights into an Old Story. *Acta Neuropathol*. 118: 723–736. doi:10.1007/s00401-009-0591-3
36. Basoglu H, Boylu NT, Kose H (2013): Cuprizone-Induced Demyelination in Wister Rats; Electrophysiological and Histological Assessment. *Eur Rev for Med Pharmacol Sci*. 17(20): 2711-2717. PMID:24174351. [www.researchgate.net/publication/258204616](http://www.researchgate.net/publication/258204616)
37. Li Z, Liu F, He X, Yang X, Shan F, Juan Feng J (2019): Exosomes Derived from Mesenchymal Stem Cells Attenuate Inflammation and Demyelination of the Central Nervous System in EAE Rats by Regulating the Polarization of Microglia. *International Immunopharmacology*. 67:268–280. doi:10.1016/j.intimp.2018.12.001
38. Gudi V, Moharreggh-Khiabania D, Skripuletz T, Paraskevi N, Koutsoudakia PN, Kotsiaria A, Skuljeca J, Trebsta C, Stangela M (2009): Regional Differences Between Grey and White Matter in Cuprizone Induced Demyelination. *Brain research*. 1 2 8 3: 1 2 7 – 1 3 8. doi: 10.1016/j.brainres.2009.06.005
39. Sachs HH, Bercury kk, Popescu DC, Narayanan SP, and Macklin WB (2014): A New Model of Cuprizone-Mediated Demyelination/Remyelination. *ASN Neuro*. 1-16. doi: 10.1177/1759091414551955
40. Leo H, Kipp M (2022): Remyelination in Multiple Sclerosis: Findings in the Cuprizone Model. *Int. J. Mol. Sci*. 23(24):1-32; 16093. doi:10.3390/ijms232416093
41. Skripuletz T, Hackstette D, Bauer K, Gudi V, Pul R, Voss E, *et al.*, (2013): Astrocytes Regulate Myelin Clearance Through Recruitment of Microglia during Cuprizone-induced Demyelination. *Brain*. 136 (1):147-67. doi: 10.1093/brain/aws262
42. Kipp M, Nyamoya S, Hochstrasser T, Amor S (2017): Multiple Sclerosis Animal Models: A Clinical and Histopathological Perspective. *Brain Pathology*. 27: 123–137. doi: 10.1111/bpa.12454
43. Gudi V, Gingele S, Skripuletz T, Stangel M (2014): Glial Response During Cuprizone-Induced De- and Remyelination in the CNS: Lessons Learned. *Front. Cell. Neurosci*. 8 (73):1-24. doi: 10.3389/fncel.2014.00073

44. Kalafatakis I, Karagogeos D (2021): Oligodendrocytes and Microglia: Key Players in Myelin Development, Damage and Repair. *Biomolecules*. 11; 1058:1-20. doi: 10.3390/biom11071058

## الملخص العربي

# دراسة هستولوجية لتأثير الإكزوسومات المشتقة من الخلايا الجذعية الوسيطة للنخاع العظمي على الجسم الثفني في نموذج فأر مصاب بالتصلب المتعدد مستحث بالكوبريزون

بوسى احمد عبد العزيز حسن، نجوى محمد الشكعة، جهاد احمد حمودة، منى حسين رافت احمد

قسم الهستولوجيا، كلية الطب، جامعة عين شمس

**المقدمة:** التصلب المتعدد هو مرض مزمن مزيل للميالين و يصيب ملايين الاشخاص في جميع أنحاء العالم. لا يوجد حالياً علاج لإعادة تكوين الميالين لهذا المرض ، ويجري استكشاف الإكزوسومات كبديل.

**الهدف:** لدراسة تأثير الإكزوسومات الناتجة من الخلايا الجذعية الوسيطة للنخاع العظمي علي بنية الجسم الثفني لنموذج كوبريزون لمرض التصلب المتعدد لذكور الفئران.

**المواد وطرق البحث:** تم استخدام سبعة واربعون من ذكور الفئران البالغة في هذا العمل ، عزلت الإكزوسومات واستخرجت من خمسة فئران . تم تقسيم الفئران الاثنتين والاربعين الي مجموعتين متساويتين بشكل عشوائي: المجموعة الاولى (المجموعة الضابطة): قسمت الي ثلاث مجموعات فرعية متساوية والمجموعة الثانية (المجموعة المعالجة بالكوبريزون): التي تم معالجتها بالكوبريزون، تلقوا ٤٠٠ مجم/كجم/يوم من الدواء عن طريق الفم يوميا لمدة ٨ اسابيع. ثم تم تقسيمهم الي ٣ مجموعات فرعية متساوية: المجموعة الفرعية الثانية- أ (كوبريزون): تم التضحية بالفئران بعد ٢٤ ساعة من آخر جرعة من الكوبريزون. المجموعة الفرعية الثانية – ب (التعافي): تركت الفئران دون علاج لمدة ٤ اسابيع ، ثم تم التضحية بهم. بعد الجرعة الاخيرة من الكوبريزون، المجموعة الفرعية الثانية – ج(المعالجة بالإكزوسومات): تلقت الفئران حقنة وريدية واحدة من الإكزوسومات عبر الوريد الذيلي ، وتمت التضحية بهم بعد ٤ اسابيع. بعد التضحية، تم تحضير أنسجة الدماغ باستخدام طرق هستولوجية و هستوكيميائية المناعية و الدراسات الهستومورفومترية.

**النتائج:** أظهر التحليل النسيجي للجسم الثفني في المجموعات الفرعية الثانية أ والثانية ب تلفا في الالياف العصبية مع العديد من فجوات صبغة الهيماتوكسولين والإيوسين . وقد لوحظ تحسن في هذه التغيرات في المجموعة الفرعية الثانية ج. باستخدام صبغة لوكسول فاست بلو، تصبغت الالياف العصبية باللون الازرق الغامق في المجموعة الضابطة و المجموعة الفرعية الثانية ج. بينما المجموعات الفرعية الثانية-أ والثانية-ب، تصبغت الالياف العصبية باللون الازرق الباهت. أظهرت المجموعات الفرعية الثانية أ والثانية ب ارتفاعا ملحوظا في عدد الخلايا إيجابية التفاعل للبروتين الحمضي الليفي الدبقي ول Iba١

**الخلاصة:** في نموذج كوبريزون للتصلب المتعدد، قد تبين أن الإكزوسومات تعمل علي تحسن ازالة الميالين من الجسم الثفني للفئران. ولذلك، قد تقدم الإكزوسومات نهجا جديدا لعلاج التصلب المتعدد.